Available online at www.sciencedirect.com
SCIENCE DIRECT®
Biochimica et Biophysica Acta 1557 (2003) 91–98
BIOCHIMICA ET BIOPHYSICA ACTA
BBA
www.bba-direct.com

The photochemical trapping rate from red spectral states in PSI–LHCI is determined by thermal activation of energy transfer to bulk chlorophylls

Robert C. Jennings*, Giuseppe Zucchelli, Roberta Croce, Flavio M. Garlaschi

Dipartimento di Biologia, Centro C.N.R. Biologia Cellulare e Molecolare delle Piante, Università di Milano, via G. Celoria, 26, 20133 Milan, Italy

Received 17 May 2002; received in revised form 9 December 2002; accepted 13 December 2002

Abstract

The average fluorescence decay lifetimes, due to reaction centre photochemical trapping, were calculated for wavelengths in the 690- to 770-nm interval from the published fluorescence decay-associated emission spectra for Photosystem I (PSI)–light-harvesting complex of Photosystem I (LHCI) [Biochemistry 39 (2000) 6341] at 280 and 170 K. For 280 K, the overall trapping time at 690 nm is 81 ps and increases with wavelength to reach 103 ps at 770 nm. For 170 K, the 690-nm value is 115 ps, increasing to 458 ps at 770 nm. This underlines the presence of kinetically limiting processes in the PSI antenna (diffusion limited). The explanation of these nonconstant values for the overall trapping time band is sought in terms of thermally activated transfer from the red absorbing states to the "bulk" acceptor chlorophyll (chl) states in the framework of the Arrhenius–Eyring theory. It is shown that the wavelength-dependent "activation energies" come out in the range between 1.35 and 2.7 kcal mol^{-1}, increasing with the emission wavelength within the interval 710–770 nm. These values are in good agreement with the Arrhenius activation energy determined for the steady-state fluorescence yield over the range 130–280 K for PSI–LHCI. We conclude that the variable trapping time in PSI–LHCI can be accounted for entirely by thermally activated transfer from the low-energy chl states to the bulk acceptor states and therefore that the position of the various red states in the PSI antenna seems not to be of significant importance. The analysis shows that the bulk antenna acceptor states are on the low-energy side of the bulk antenna absorption band.

Keywords: Photochemical trapping; Thermal activation; Chlorophyll

1. Introduction

Photosystem I (PSI) of higher plants is a supramolecular pigment/protein complex, localised in the nonappressed regions of thylakoid membranes. The complex binds the primary electron donor chlorophylls (chls), known as P700, and can photoreduce ferredoxin using plastocyanin and cytochromes as secondary electron donors [1]. The complex has two moieties, which are the central chl *a*-binding core complex and a peripheral antenna which consists of four light-harvesting complex of PSI (LHCI) chl *a*/*b* binding proteins. The core complex binds approximately 90–100 chl *a* and probably about 20 β-carotene molecules [2,3] as well as P700 and the primary acceptors A0 and A1 at the interface between the two homologous subunits [4]. The LHCI complexes seem to be arranged on one side of the core [5] and, taken together, they bind about 80–100 chl *a*+*b* molecules and 20 xanthophylls, with the number of complexes surrounding the core probably being around 10. The LHCI complexes are thought to bind on average eight chl *a* and two chl *b* molecules [6].

The PSI–LHCI complex can be isolated in an intact form, that is, without detergent solubilised chls present [7]. In the region of the lowest lying electronic transition (Q_y), the complex has a broad absorption band with its maximum at 680 nm. This band is associated with the so-called "bulk" antenna chl *a* and accounts for about 180 chl *a* molecules. Owing to the broadness of this band, the approximately 20 chl *b* molecules cannot be resolved in absorption spectra, even at cryogenic temperatures. However, it is known that their Q_y transition is near 650 nm from analysis of the isolated LHCI complexes [8]. A peculiarity of the PSI–LHCI absorption spectrum is the presence of significant absorption in the low-energy tail, indicating the presence of red spectral chl *a* forms, or states, absorbing at energies lower than that of the primary donor P700. Their combined oscillator strength is approximately equivalent to 10 chls [7].

Abbreviations: chl, chlorophyll; DAS, decay-associated spectra; LHCI, light-harvesting complex of Photosystem I; PSI, Photosystem I; P700, Photosystem I primary electron donor

* Corresponding author. Tel.: +39-2-298-631; fax: +39-2-5031-4815.
E-mail address: Robert.Jennings@unimi.it (R.C. Jennings).

0005-2728/02/$ - see front matter © 2002 Elsevier Science B.V. All rights reserved.
doi:10.1016/S0005-2728(02)00399-7

Though the PSI–LHCI absorption is structureless in this low-energy region, even at cryogenic temperatures, the fluorescence spectra are not. From a combination of steady-state and time-resolved fluorescence measurements, a minimum number of three and possibly four distinct spectral forms have been detected [7,9], with emission maxima near 720, 730, and 740–745 nm. The absorption origin bands of these red forms are not known with certainty though hole burning and thermal broadening absorption spectroscopies indicate that the electron/phonon coupling of red forms is much stronger than for the bulk antenna chls [8,10,11] and suggest that their Stokes shifts are in the 6- to 10-nm range. It is thought that the large bathochromic spectral shifts of red forms may be due to strong Coulombic interactions with other chlorophyll molecules, leading to excitonic band splitting, with the red forms representing the low-energy excitonic band of chl dimers. Direct evidence, from pump probe anisotropy experiments and circular dichroism measurements, in favour of this, has been presented for a red form absorbing near 709 nm in *Synechocystis* and *Spirulina* core complexes [12,13]. In both of these cases, the high-energy excitonic band is in the bulk chl *a* antenna absorption region. However, it should be pointed out that in the *Spirulina* trimers, there are several red absorbing states on the long wavelength side of the 709-nm band [13–15] which do not give rise to a circular dichroism signal [13], thus suggesting the possibility that not all red forms arise from strong excitonic interactions. In LHCI, their formation seems to require the presence of chl *b*, as indicated by reconstitution experiments in which pigments were bound to the apoprotein in vitro [16], though its exact function is not known.

The biological role of these low-energy chls has been much debated over the years. It is now fairly generally accepted that this is not to be sought in terms of increasing the rate of energy flow from the antenna to the primary donor chls [9,17–20]. In fact, it has been experimentally demonstrated, from time-resolved fluorescence experiments in both cyanobacterial core complexes and PSI–LHCI, that the red forms slow down energy flow into the reaction centre due to their own trapping function and the slow, energetically uphill energy flow from them to P700 [9,19,20]. The recent demonstration [21] that the red forms have an important light-harvesting function in dense vegetation systems, where the ambient light spectral composition is enriched in wavelengths above 690 nm with respect to normal daylight, seems to be the most likely function for these chl forms. In this context, it is obviously important that the cost/benefit relation should not be too high, that is, that the slow, energetically uphill, energy transfer to the bulk chls should not be so slow as to significantly lower the quantum efficiency of primary reaction centre trapping [7,22,23].

Information on the dynamics of energy trapping from the red chl forms are available from time-resolved fluorescence experiments. For an intact PSI–LHCI preparation, analysed both in terms of the decay-associated spectra (DAS) and the time-resolved emission spectra (TRES), it was demonstrated that spectral red shifting occurs during the entire fluorescence decay [9]. This implies that the trapping time is not constant across the red emission region. A similar situation may be adduced from an earlier study on plant PSI–LHCI [24]. As approximately 80–90% of antenna excited states are transferred to the red forms before photochemical trapping [7,9], it is important to understand this aspect. In principle, different trapping times (τ_{tr}) across the red emission band could be caused by: (i) positional effects, whereby different red forms are present in different antenna domains, such as the core antenna or different LHCI antenna complexes, with different transfer rates being associated; (ii) differential thermal activation for energy transfer from the different red absorbing states to specific bulk antenna acceptors before trapping; and (iii) a combination of (i) and (ii). In the present paper, we analyse this important point using PSI–LHCI particles. From our previously published time resolved data [9], the values of τ_{tr} between 710 and 770 nm for 280 and 170 K have been calculated. At both temperatures, the trapping time increases across the red absorption/fluorescence tail with values ranging from 81 to 103 ps at 280 K and from 115 to 458 ps at 170 K for the wavelength interval 690–770 nm. It is furthermore demonstrated that, when these data are analysed by means of Arrhenius–Eyring theory, the thermal activation energies for trapping over the red emission band between 710 and 780 nm come out in the range 1.35–2.7 kcal mol^{-1}, with the higher values correlating with the longer wavelengths. These values are shown to fall around the "average" activation energy (2 kcal mol^{-1}) for the fluorescence yield of the red forms in this temperature range, determined by the phenomenological Arrhenius plot, thus indicating that it is the thermal energy barrier which is dominant in determining the dynamics of trapping from the red forms. The mean energy levels of the bulk antenna forms which function as excitation energy acceptors for the red chl states are also determined and are found to lie on the low-energy side of the bulk antenna absorption band.

2. Materials and methods

The PSI–LHCI complex was prepared using the octyl β-D-glucopyranoside method as previously described [7]. The chl *a*/*b* ratio of the preparation was between 11.6 and 12. Steady-state fluorescence spectra were measured in an EG&G OMAIII (Model 1460) between 70 and 280 K as previously described [7]. Spectra were corrected for instrumental distortion using an intensity calibrated source (ISCO Spectroradiometer). Picosecond time-resolved fluorescence data are taken from our previous study [9]. These measurements were performed in the presence of sodium ascorbate/PMS to maintain P700 in a reduced state and an oxygen scavenger system to avoid oxygen effects. The emission decays were recorded every 10 nm between 690 and 780 nm and analysed by global analysis methods [25].

3. Results and discussion

Our aim is to study energy transfer from the red absorbing states in PSI–LHCI to the primary photochemical trap, P700. As most of the red forms in PSI–LHCI seem to be localised in the outer antenna complexes (LHCI) [8], and hence physically distant from P700, it is reasonable to expect that energy transfer from them will be to bulk chls and not to the primary trap itself. It may be noted, however, that due to the unusually strong electron–phonon coupling suggested for P700 [26], at the temperatures used in these experiments, there is considerable spectral overlap between the thermally broadened Q_y(0,0) absorption transition of P700 and the long wavelength absorbing antenna states (Fig. 1). In Fig. 1, the band width (approximately 20 nm) and band symmetry for P700 are those expected in the linear electron/phonon coupling assumption for the reported coupling strength [26], at this temperature. Thus, from a purely energetic viewpoint, the high-energy, bulk, chls need not always be involved.

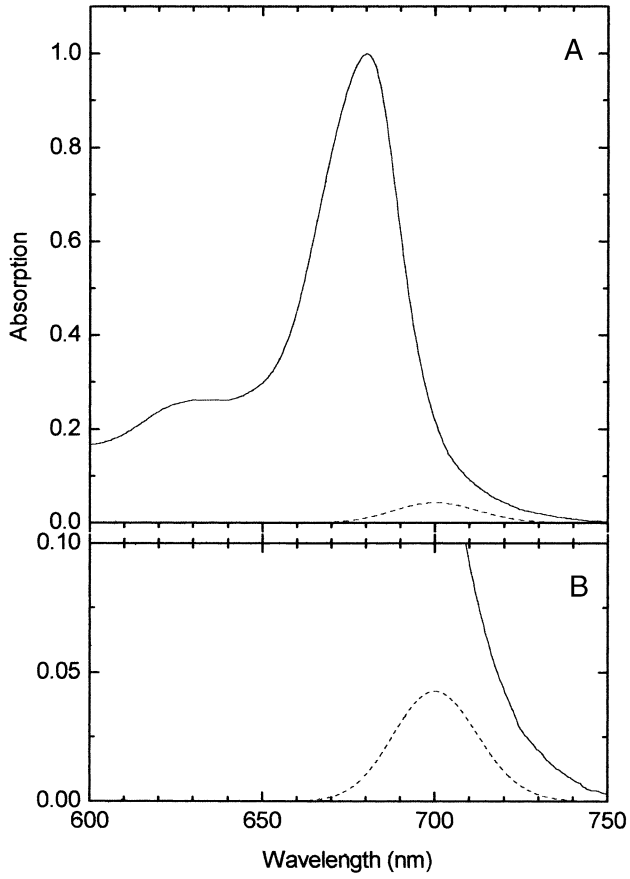

Fig. 1. Electronic absorption spectrum of PSI–LHCI, in the Q_y region (solid line) at 280 K, and the calculated spectrum for the thermally broadened Q_y(0,0) of P700 (dashed line) at 280 K, assuming a Gaussian function and using the measured [26] electron/phonon coupling values ($S=5$, $\nu_m=30$ cm^{-1}) for P700, with an inhomogeneous site distribution of 130 cm^{-1} (full width at half-maximum) to determine its total width. In panel B, the absorption scale is expanded to show more clearly the expected distribution of the Q_y(0,0) absorption for P700.

To determine the values of τ_{tr} for the red absorbing states, we have used the time-resolved fluorescence data for PSI–LHCI, previously published by some of us [9]. These data allow determination of a characteristic, ensemble lifetime value, for the fluorescence decay profile at each wavelength and, as the measurements were performed with active reaction centres, this value is directly related to the photochemical trapping time. The complete set of DAS is presented in Fig. 2 of that paper for 280 and 170 K. As discussed previously [9], at 280 K, four components are resolved, with lifetimes of 11, 57, 130, and 769 ps. The 769-ps component, which has very low amplitudes, represents an extremely low amount of chl which is weakly coupled to the PSI–LHCI chl matrix and will be ignored in the following analysis. The 11-ps component, with both positive and negative amplitudes, represents energy flow from the bulk pigments to the red forms. Faster energy transfer components of this kind, unresolved in these experiments, are present, as the red states are strongly populated in less than 11 ps. For cyanobacteria, an approximately 4-ps transfer component was detected in experiments with greater time resolution by Gobets et al. [20]. The 57- and 130-ps decays have only positive amplitudes, presented here in Fig. 2A, thus indicating that they are pure trapping components. At 170 K, four DAS components were resolved. The fastest has a lifetime of 10 ps and displays both positive and negative DAS amplitudes, which indicates that it represents transfer from the bulk into the red absorbing states. Also at this temperature, the red states are strongly populated in less than 10 ps, which indicates the presence of unresolved transfer components. The other three components (55, 216, and 715 ps) have only positive amplitudes (Fig. 2B), thus indicating that they represent trapping. In the following, we will use these trapping components at both temperatures to calculate the spectrum of the trapping time (τ_{tr_λ}) where $\tau_{tr_\lambda}=(\Sigma A_{i\lambda}\tau_{i\lambda})/\Sigma A_{i\lambda}$, where $A_{i\lambda}$ and $\tau_{i\lambda}$ are the DAS amplitudes and lifetimes of the trapping components at each wavelength. That this is the correct lifetime parameter to describe the trapping of antenna excited states is demonstrated in Appendix A (see also Lakowitz [27]).

We have not considered the 10-ps transfer component in these calculations, even though its line shape is nonconservative, which could indicate a small amount of trapping directly from bulk chls (< 5% of total trapping). However, a similar, nonconservative component has been observed by Gobets et al. [20] with LHCI preparations, in which trapping does not occur. Thus, the reason for the nonconservative line shape of this DAS is not clear. The origin of multiple decay components with only positive amplitudes is not understood at the moment. It is possible that they reflect trapping from different antenna domains ("position effect") or the presence of reversible reactions at the level of primary electron transfer.

The trapping time spectra (τ_{tr_λ}) are presented in Fig. 3. At both temperatures, there is a significant increase in this parameter with increasing emission wavelength (81–103

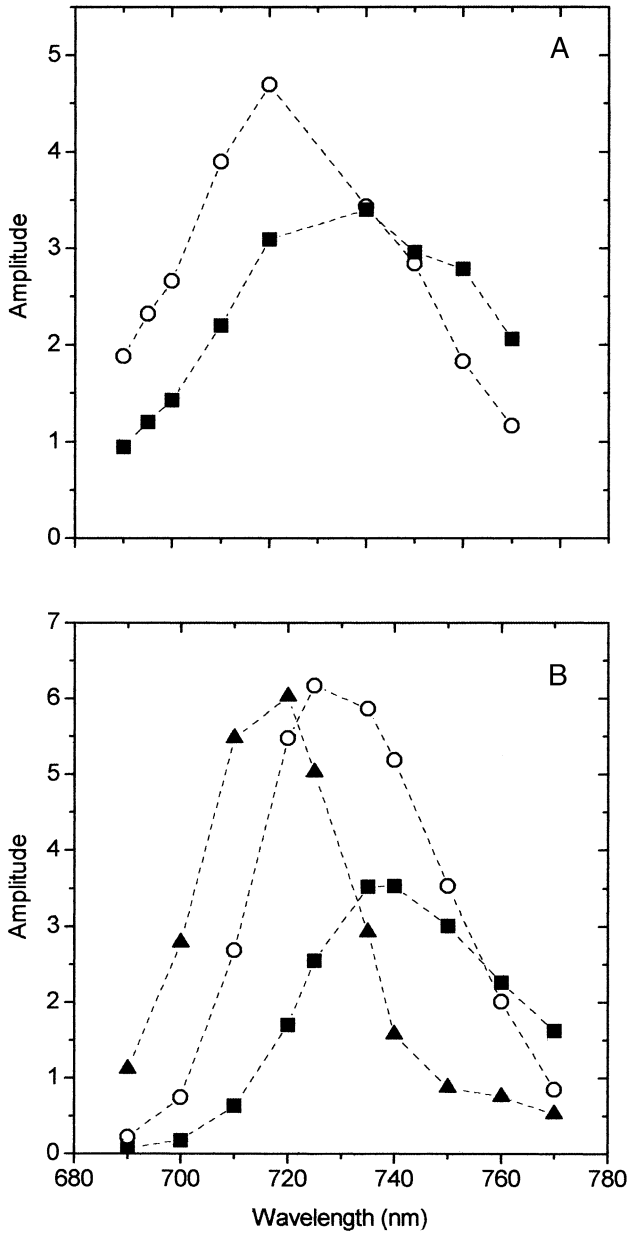

Fig. 2. The DAS of the 57- and 130-ps fluorescence decay components of PSI–LHCI measured at 280 K (A) and the 55-, 216-, and 715-ps components measured at 170 K (B).

ps at 280 K; 115–458 ps at 170 K). This effect, which is much greater at the lower temperature, suggests that a thermal activation component is involved, and furthermore underlines the presence of kinetically limiting processes in the PSI antenna (diffusion limited).

We now address the question of the physical reason for these nonconstant values for τ_{tr}. Two possibilities present themselves. First, they could in principle be associated with a positional effect of the red states in the PSI antenna where the different red states are physically present in different antenna domains which transfer to the reaction centre with different rates. Second, they could be due to thermally activated uphill energy transfer to bulk pigments, with different thermal "activation" energies for the different red states. Our approach has been to examine the second possibility in detail. This is achieved by determination of the phenomenological Arrhenius activation energy for steady-state fluorescence emission from PSI–LHCI which is compared with the set of values obtained by analysing the τ_{tr} data using Arrhenius–Eyring theory. If thermal activation is important for determining the nonconstant values for τ_{tr}, then we expect close agreement between the two time-resolved data sets, obtained at 170 and 280 K and the activation energy determined from the steady-state fluorescence data, that is, the analyses based on Eqs. (3), (4), and (1), respectively. On the other hand, if the nonconstant τ_{tr} values are due largely to a "positional" effect, the time-resolved analysis (Eqs. (3)

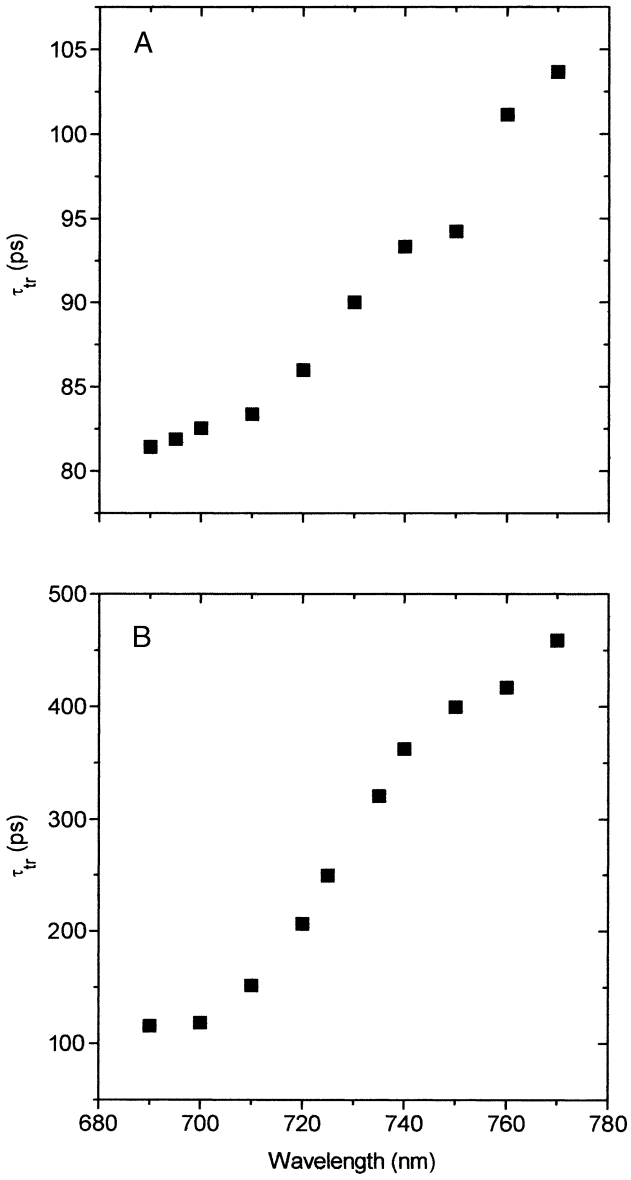

Fig. 3. The overall trapping time (τ_{tr}) for PSI–LHCI, calculated from the DAS of Fig. 2, in the wavelength interval 690–770 nm for 280 K (A) and 170 K (B).

and (4)) will not yield a result compatible with the steady-state fluorescence data (Eq. (1)).

It is well known that the fluorescence yield of PSI increases markedly as the temperature is lowered and this has been analysed in terms of Arrhenius theory by several authors [28–31]. As primary photochemistry is essentially "activationless", these experiments are interpreted in terms of energy transfer from the red states to the primary trap, where the Arrhenius activation energy represents the phonon energy necessary for energy transfer to the primary trap. We have repeated this experiment for PSI–LHCI (Fig. 4), where the temperature dependency of the fluorescence yield for PSI–LHCI is shown as a simple Arrhenius plot (Eq. (1)) in which the fluorescence yield (F) was determined from the integrated areas under the emission curves between 650 and 780 nm:

$$\ln F = \ln A - E_a/RT \quad (1)$$

A is the Arrhenius pre-exponential term; E_a is the phenomenological Arrhenius activation energy; and R and T have their usual meaning. The data are well described by a straight line down to 125 K, though some deviation occurs at lower temperatures, in agreement with Pålsson et al. [30]. For the 125- to 280-K interval, a thermal activation energy (E_a) of 2 kcal mol^{-1} (690 cm^{-1}) is determined. Though this value is higher than those previously reported for cyanobacteria [28–30], it is apparently not unreasonable as the fluorescence emission peak at RT is near 730 nm (13 699 cm^{-1}) and a shift of 690 cm^{-1} on the high-energy side corresponds to 695 nm, that is, within the bulk antenna absorption band. This difference with respect to the cyanobacterial core systems may

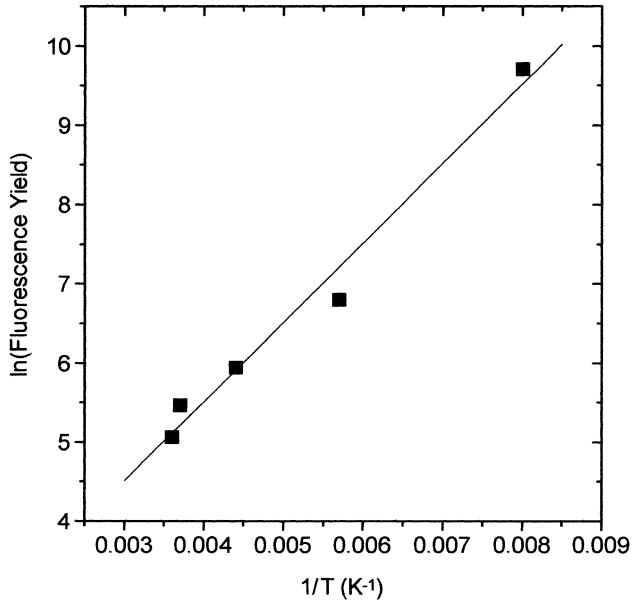

Fig. 4. Arrhenius plot of the fluorescence yield of PSI–LHCI, determined as the integrated area subtended by the steady-state fluorescence emission spectra profiles between 650 and 800 nm.

reflect different energy transfer pathways from the red states to P700 in PSI–LHCI, where most of the red forms are associated with the external antenna complexes [8]. However, it should be pointed out that an exact interpretation from this kind of analysis is not possible when there are multiple red absorbing states, which is nearly always the case. This is because each state may be associated with a different thermal activation energy. Thus, the Arrhenius activation energy of 2 kcal mol^{-1} can only be interpreted as a kind of average value for the whole population of red forms. In the present context, however, this is useful as it provides a reference point for the emission wavelength-dependent values obtained below using Arrhenius–Eyring theory. We are aware that excited energy transfer out of the red absorbing states is expected to proceed via the Förster mechanism in which such factors as dipole orientation, centre-to-centre distance, and the so-called Förster overlap integral are involved. Of these transfer micro-parameters, it is only the overlap integral which displays a temperature dependency due to the coupling of excited state electrons to the phonon bath. To analyse thermal activation in terms of the Förster theory, it would therefore be necessary to have detailed information on the band shapes of both the long wavelength donor state and the bulk acceptor states. Such information is not at present available. We have therefore chosen to analyse this process in terms of the Arrhenius–Eyring transition state theory and assume that energy transfer from the red absorbing states is into bulk chl acceptor states, which are characterised by higher, or possibly approximately equal, energy levels to that of the primary donor, P700. We envisage the "transition state complex" as the Coulombic coupled state of the transition dipoles of donor and acceptor molecules. Thermal activation and attainment of the transition state complex involves broadening of the optical donor/acceptor bands leading to nonzero values for the Förster overlap integrals. It should be noted that the distance and orientation terms in the Förster theory are entropic in nature and may be considered to not change during energy transfer from the red states to the high-energy bulk chl acceptors. Thus, the "entropy of activation" is zero, as will be further underlined below.

To proceed with this approach, it is necessary to establish the overall transfer rates from the red forms to the bulk chls. As 690 nm is the peak emission wavelength of the bulk chls, the trapping time for an excited state in these pigments is therefore expected to be close to 81 ps in PSI–LHCI at 280 K and 115 ps at 170 K. This parameter will be defined as τ_{tr_b} and depends both on the rate of excitation migration to the primary trap and on the rate of primary photochemistry, which in the simplified case of an isoenergetic pigment lattice, is given by Eq. (2) [32,33]:

$$\tau_{tr_b} = \tau_{mig} + \tau_{cs} \quad (2)$$

where τ_{tr_b} is the overall trapping time, τ_{mig} is the migration time from the antenna to the primary trap, and τ_{cs} is the charge separation time from the primary trap excited state. If

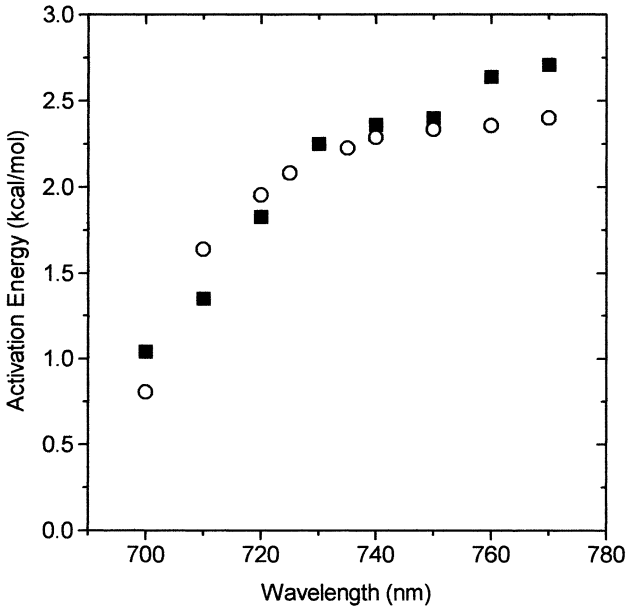

Fig. 5. The activation energy for primary photochemical trapping by PSI–LHCI in the wavelength interval 700–770 nm, calculated according to Eq. (4), at 280 K (squares) and at 170 K (circles).

we now make the assumption that τ_{tr_b} is constant for excited states no matter where they physically reside in the bulk antenna, then it is reasonable to associate the increased values for the trapping time from the red absorbing states (τ_{r_λ}) with the overall transfer time from these states to the high-energy bulk chls. Thus, we have $\tau_{r_\lambda} = \tau_{tr_\lambda} - \tau_{tr_b}$. In the following, we have used $(\tau_{r_\lambda})^{-1}$ to indicate the collection of energy transfer rates from the red absorbing states to the bulk chls. We have considered emission wavelengths from 710 to 770 nm with data points separated by 10 nm. Our aim is to find the thermal activation energy over this wavelength interval. To this end, we use the Eyring modification [34] of the Arrhenius equation (Eq. (3)).

$$(\tau_{r_\lambda})^{-1} = (kT/h)e^{\Delta S/R}e^{-\Delta H/RT} \quad (3)$$

where ΔS and ΔH are the entropy and enthalpy of activation, respectively; k and h are the Boltzmann and Planck constants, respectively; and R is the gas constant and T the absolute temperature. In this case, the entropy and enthalpy terms refer to the parameter changes during the thermally assisted transfer from the red state to a high-energy bulk antenna chl. As the thermal energy (Δq) is taken up by the pigments from the protein–phonon bath in which they are embedded, from a completely thermalised state, at temperature T, the total entropy change ($\Delta S = \Delta q/T$) of the pigment/protein is zero. Thus, Eq. (3) simplifies to

$$(\tau_{r_\lambda})^{-1} = (kT/h)e^{-\Delta H/RT} \quad (4)$$

The enthalpy of activation, here equivalent to the free energy of activation, represents the mean energy difference between the red states and the acceptor bulk chls. From the collection of τ_{r_λ}, the ΔH (ΔG) of activation at both temperatures was determined (Fig. 5). For the wavelength interval associated with the red forms (710–770 nm), the ΔH of activation increases from 1.35 kcal mol^{-1} at 710 nm to 2.4–2.7 kcal mol^{-1} at 770 nm. Agreement between the data sets for the two temperatures (170 and 280 K) is good, which clearly justifies the approach used. It is evident that these values lie around the value of 2 kcal mol^{-1} obtained from the steady-state fluorescence measurements (Fig. 4). In fact, the fluorescence amplitude weighted sum of these values for the different wavelengths ($\Sigma F_\lambda \Delta H_\lambda / \Sigma F_\lambda$) yields a value of 2.05 kcal mol^{-1} when both temperatures are considered together. Thus, we conclude that the nonconstant τ_{r_λ} over the long wavelength absorption/fluorescence wing of PSI–LHCI can be entirely explained in terms of different thermal activation energies for the uphill energy transfer to bulk acceptor molecules. It would seem that the position effect is not significant.

If this approach is correct, then it is possible to determine the upper limit for the mean energy levels of the bulk acceptor states (Eb_λ) for each of the long wavelength donor states (Er_λ), as the excited state acceptor state is expected to lie at energies either equal to or below that of the transition state complex. The data are presented in Fig. 6. For the lowest energy transitions ($Er_\lambda = 750–770$ nm), transfer is into energy levels at, or lower than ($Eb_\lambda = 705–718$ nm), values which are clearly outside the main bulk chl band, as this is maximal at 680 nm (Fig. 1) and has an approximate half-bandwidth of 15 nm on the long wavelength side and 25 nm on the short wavelength side. These energy levels can be seen to overlap with the low-energy side of the thermally

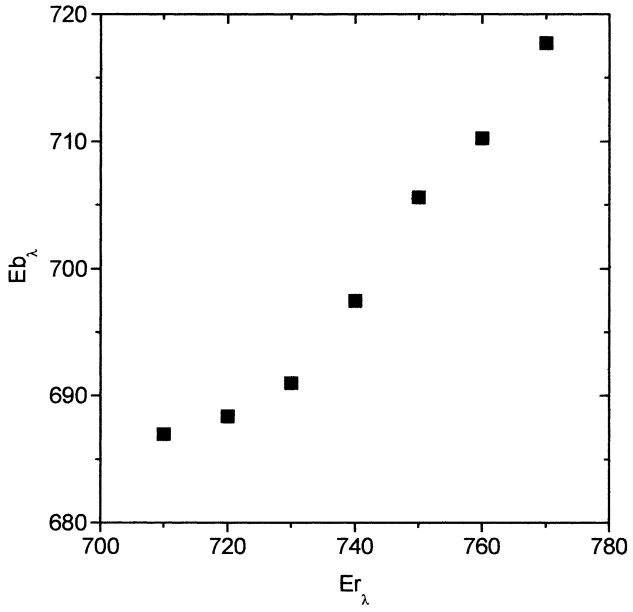

Fig. 6. Plot of the maximum values for the mean energy levels of the bulk chlorophyll acceptor states (Eb_λ), expressed in nanometers, for energy transfer from the long wavelength antenna states (Er_λ) for 280 K. Data are derived from the thermal activation energies for trapping of Fig. 3.

broadened Q_y band of P700 (Fig. 1) and thus may be interpreted as transfer into the small population of antenna states which are approximately isoenergetic with P700 (Fig. 1). For the higher energy red states (Er_λ = 710–740 nm), transfer occurs to states with transitions lying between 700 and 680 nm (Eb_λ), or lower. This analysis therefore indicates that the excited states of the red forms are thermally transferred into antenna states absorbing on the low-energy side of the bulk antenna energy distribution. This conclusion is, of course, not unreasonable as transfer into the high-energy side of the bulk antenna energy distribution would require even greater thermal activation energies with a consequent further slowing down of the "uphill" transfer process into the bulk antenna. This conclusion is not in agreement with the earlier suggestion [35] that the red forms transfer preferentially into chl *b*, which absorbs near 650 nm in PSI [8].

The present conclusions are relevant to the modelling of PSI excitation dynamics by means of compartment-based models. In these models, detailed energy balance is invariably considered, taking into account the mean energy level of the compartment and its degeneracy. Thus, for energy transfer from the red absorbing states to the bulk chls, the mean energy of the bulk chls is used. From the present study, it would appear that this approach has serious shortcomings, particularly when the model is used to describe data over a range of temperature values. In this case, detailed energy balance between the compartments should consider the red chl donor state and the bulk chl acceptor state and not the mean energy levels of the compartments.

Appendix A

In a multicomponent system which decays due to the presence of a trap, the choice of the lifetime parameter which accurately represents the overall trapping time is not immediately obvious. Basically, two possibilities exist:

(i) the mean lifetime value (τ_m), where $\tau_m = \sum_j A_j\tau_j^2 / \sum_j A_j\tau_j$. This is the first central moment of the multi-exponential decay (centre of gravity);
(ii) the parameter which is often referred to as the "average" lifetime (τ_{av}), where $\tau_{av} = \sum_j A_j\tau_j / \sum_j A_j$.

In the following, we demonstrate that τ_{av} is the correct choice.

For a simple, two-level system coupled by first-order rate processes and in which the initially populated state is *A* (see below), analytical solutions for the eigenvalues and eigenvectors are readily available (Eqs. (A1)–(A4)).

$$A \underset{k_{-1}}{\overset{k_1}{\rightleftarrows}} B \xrightarrow{k_2}$$

$$\tau_1^{-1} = 0.5[(k_1 + k_{-1} + k_2) + ((k_1 - k_{-1} - k_2)^2 + 4k_1k_{-1})^{0.5}] \quad (A1)$$

$$\tau_2^{-1} = 0.5[(k_1 + k_{-1} + k_2) - ((k_1 - k_{-1} - k_2)^2 + 4k_1k_{-1})^{0.5}] \quad (A2)$$

$$A_1 = (\tau_1^{-1} - k_{-1} - k_2)/(\tau_1^{-1} - \tau_2^{-1}) \quad (A3)$$

$$A_2 = (\tau_2^{-1} - k_{-1} - k_2)/(\tau_2^{-1} - \tau_1^{-1}) \quad (A4)$$

where τ_1^{-1} and τ_2^{-1} are the two decay lifetimes and A_1 and A_2 are their respective amplitudes.

From these analytical solutions, it can easily be shown that:

$$\tau_{av}^{-1} = [(A_1\tau_1 + A_2\tau_2)/(A_1 + A_2)]^{-1} = k_1k_2/(k_{-1} + k_2) \quad (A5)$$

The overall rate of depopulation of the two-level kinetic system is given by $= k_2[B]_t$, where $[B]_t$ is the concentration of *B* at any time. For the steady state, $[B]_{ss} = k_1[A]_{ss}/(k_{-1} + k_2)$ and the overall rate is then given by $k_1k_2[A]_{ss}/(k_{-1} + k_2)$ which from Eq. (A5) is $\tau_{av}^{-1}[A]_t$. Thus, it is clear that τ_{av}^{-1} can be considered the effective rate constant for depopulation of the *A* level.

References

[1] B.D. Bruce, R. Malkin, J. Biol. Chem. 263 (1988) 7302–7308.
[2] R.C. Jennings, R. Bassi, G. Zucchelli, Top. Curr. Chem. 177 (1996) 147–181.
[3] P. Jordan, P. Fromme, H.T. Witt, O. Klukas, W. Saenger, N. Krauss, Nature 411 (2001) 909–917.
[4] J.H. Golbeck, Annu. Rev. Plant Physiol. Plant Mol. Biol. 43 (1992) 293–324.
[5] E.J. Boekema, P.E. Jensen, E. Schlodder, J.F.L. van Breemen, H. van Roon, H.V. Scheller, J.P. Dekker, Biochemistry 40 (2001) 1029–1036.
[6] R. Croce, R. Bassi, in: G. Garab (Ed.), Photosynthesis: Mechanisms and Effects, vol. 1, Kluwer Academic Publishers, Dordrecht, 1998, pp. 421–424.
[7] R. Croce, G. Zucchelli, F.M. Garlaschi, R. Bassi, R.C. Jennings, Biochemistry 35 (1996) 8572–8579.
[8] R. Croce, G. Zucchelli, F.M. Garlaschi, R.C. Jennings, Biochemistry 37 (1998) 17355–17360.
[9] R. Croce, D. Dorra, A.R. Holzwarth, R.C. Jennings, Biochemistry 39 (2000) 6341–6348.
[10] A. Cometta, G. Zucchelli, N.V. Karapetyan, E. Engelmann, F.M. Garlaschi, R.C. Jennings, Biophys. J. 79 (2000) 3235–3243.
[11] M. Ratsep, T.W. Johnson, P.R. Chitnis, G.J. Small, J. Phys. Chem., B 104 (2000) 836–847.
[12] S. Savikhin, W. Xu, V. Soukoulis, P.R. Chitnis, W.S. Struve, Biophys. J. 76 (1999) 3278–3288.
[13] E. Engelmann, T. Tagliabue, N.V. Karapetyan, F.M. Garlaschi, G. Zucchelli, R.C. Jennings, FEBS Lett. 499 (2001) 112–115.
[14] N.V. Karapetyan, D. Dorra, G. Schweitzer, I.N. Bezsmertnaya, A.R. Holzwarth, Biochemistry 36 (1997) 13830–13837.
[15] B. Koehne, H.W. Trissl, Biochemistry 37 (1998) 5494–5500.
[16] V.H.R. Schmid, P. Thome, W. Ruhle, H. Paulsen, W. Kuhlbrandt, H. Rogl, FEBS Lett. 499 (2001) 27–31.
[17] M.R. Fischer, A.J. Hoff, Biophys. J. 63 (1992) 911–916.

[18] H.W. Trissl, Photosynth. Res. 35 (1993) 247–263.
[19] M. Byrdin, I. Rimke, E. Schlodder, D. Stehlik, T.A. Roelofs, Biophys. J. 79 (2000) 992–1007.
[20] D. Gobets, I.H.M. van Stokkum, M. Rogner, J. Kruip, E. Schlodder, N.V. Karapetyan, J.P. Dekker, R. van Grondelle, Biophys. J. 81 (2001) 407–424.
[21] A. Rivadossi, G. Zucchelli, F.M. Garlaschi, R.C. Jennings, Photosynth. Res. 60 (1999) 209–215.
[22] H.W. Trissl, B. Hecks, K. Wulf, Photochem. Photobiol. 57 (1993) 108–112.
[23] V.V. Shubin, I.N. Bezsmertnaya, N.V. Karapetyan, J. Photochem. Photobiol., B Biol. 30 (1995) 153–160.
[24] S. Turconi, N. Weber, G. Schweitzer, H. Strotmann, A.R. Holzwarth, Biochim. Biophys. Acta 1187 (1994) 324–334.
[25] J. Wendler, A.R. Holzwarth, Biophys. J. 52 (1987) 717–728.
[26] R. Jankowiak, J.M. Hayes, G.J. Small, Chem. Rev. 93 (1993) 1471–1502.
[27] J.R. Lakowitz, Principles of Fluorescence Spectroscopy, Kluwer Academic/Plenum Publishers, New York, 1999.
[28] V.B. Tusov, B.N. Korvatovskii, V.Z. Paschenko, L.B. Rubin, Dok. Biophys. 252 (1980) 112–115.
[29] B.P. Wittmershaus, V.M. Woolf, W.F.J. Vermaas, Photosynth. Res. 31 (1992) 75–87.
[30] L.O. Pålsson, C. Flemming, B. Gobets, R. van Grondelle, J.P. Dekker, E. Schlodder, Biophys. J. 74 (1998) 2611–2622.
[31] F. Jelezko, C. Tietz, U. Gerken, J. Wrachtrup, R. Bittl, J. Phys. Chem., B 104 (2000) 8093–8096.
[32] R.M. Pearlstein, Photochem. Photobiol. 35 (1982) 835–844.
[33] S. Kudzmauskas, L. Valkunas, A.Y. Borisov, J. Theor. Biol. 105 (1983) 13–23.
[34] H. Eyring, Chem. Rev. 17 (1935) 65–77.
[35] I. Mukerji, K. Sauer, in: M. Baltscheffsky (Ed.), Current Research in Photosynthesis, vol. II, Kluwer Academic Publishers, Dordrecht, 1990, pp. 321–324.